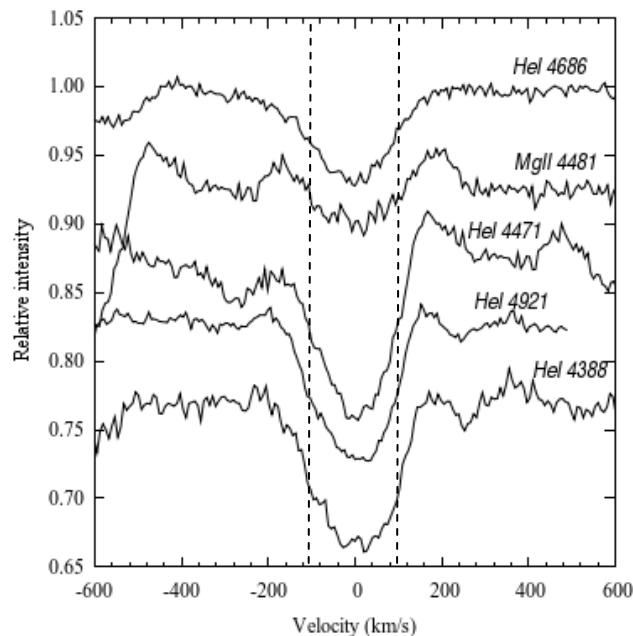


## 5.5 THE PHOTOSPHERIC LINES

In the blue region of the spectrum of  $\delta$ -Sco, we detected the following absorption lines called photospheric lines: *HeI*  $\lambda$ 4388, 4471, 4921, 4713, *MgII*  $\lambda$ 4481, *HeII*  $\lambda$ 4686, *OII*  $\lambda$ 4416, 4650, 4662, *SiII*  $\lambda$ 4553, 4568, 4576. For this study, we only analysed *HeI*  $\lambda$ 4388, 4471, 4921, *MgII*  $\lambda$ 4481 and *HeII*  $\lambda$ 4686. One of the important issues in Be stars is the rotational velocity of the star. Through a certain technique, the measurement of the photospheric lines can lead to a calculation of the rotational velocity of the star, because these lines originate from its photospheric layer. However, in this study, we were only studying the variation of the *FWHM* value. Although photospheric lines come from a region close to the star, some of them might still be affected by the emission lines. Table 5.4 lists the parameters of the line profiles of *EW* and *FWHM* of several photospheric lines for this study. The *FWHM* values for the photospheric lines were derived under a Gaussian distribution.



**Figure 5.24** – Dashed lines denote the estimation of *FWHM* on some of the photospheric lines.

**Table 5.4** – *EW* and *FWHM* of *HeI*  $\lambda$ 4388, 4471, 4921, *MgII*  $\lambda$ 4481, and *HeII*  $\lambda$ 4686. Column 2 and 3 show the observation dates. Column 5 and 6, respectively show the *EW* and *FWHM* values in Angstrom. Column 7 is the *FWHM* in the units of km/s.

Delta Scorpii: Photospheric lines

Line	Date	MHJD+ 2454000	EW (A)	FWHM (A)	FWHM (km/s)
<b>HeI <math>\lambda</math> 4388</b>	20090317	907.66	0.40	3.10	211.95
	20090503	954.60	0.43	3.59	245.45
	20100221	1248.72	0.36	2.98	203.74
	20100313	1268.64	0.42	3.40	232.46
	20100411	1297.60	0.37	3.43	234.51
	20100415	1301.55	0.48	4.37	298.77
	20100522	1339.44	0.30	2.81	192.12
	20100604	1352.44	0.30	3.25	222.20
	20100624	1372.40	0.40	4.14	283.05
	20100704	1382.40	0.36	3.16	216.05
	20100718	1396.37	0.32	3.48	237.93
	20100830	1439.31	0.38	3.94	269.38
	<b>MgII <math>\lambda</math> 4481</b>	20080717	665.39	0.17	2.65
20080724		672.40	0.16	3.06	204.86
20090317		907.66	0.21	3.37	225.61
20090503		954.60	0.18	3.76	251.72
20100221		1248.72	0.15	3.03	202.85
20100313		1268.64	0.18	3.57	239.00
20100411		1297.60	0.11	2.97	198.83
20100415		1301.55	0.13	3.09	206.87
20100522		1339.44	0.14	2.81	188.12
20100624		1372.40	0.09	2.50	167.37
20100704		1382.40	0.12	2.83	189.46
20100707		1385.40	0.10	2.63	176.07
20100718		1396.37	0.08	2.87	192.14
20100830	1439.31	0.09	2.54	170.05	
<b>HeII <math>\lambda</math> 4686</b>	20080709	657.48	0.22	3.07	196.56
	20080717	665.39	0.23	3.05	195.27
	20080724	672.40	0.19	2.84	181.83
	20090327	917.64	0.25	3.02	193.35
	20090418	940.52	0.19	3.10	198.48
	20090503	954.60	0.23	3.24	207.44
	20100221	1248.72	0.25	3.30	211.28
	20100313	1268.64	0.21	3.11	199.12
	20100411	1297.60	0.23	3.28	210.00
	20100415	1301.55	0.21	3.08	197.20
	20100522	1339.44	0.23	3.32	212.56
	20100604	1352.44	0.19	3.06	195.92
	20100624	1372.40	0.16	2.93	187.59
	20100704	1382.40	0.18	2.81	179.91
	20100707	1385.40	0.19	3.26	208.72
	20100718	1396.37	0.15	3.17	202.96
	20100830	1439.31	0.18	3.33	213.20
20100903	1443.30	0.15	3.00	192.07	

**Table 5.4** - Continue

Delta Scorpii: Photospheric lines

Line	Date	MHJD+ 2454000	EW (Å)	FWHM (Å)	FWHM (km/s)
<b>HeI <math>\lambda</math> 4921</b>	20090317	907.66	0.36	3.51	213.94
	20090503	954.60	0.38	3.82	232.84
	20100313	1268.64	0.39	3.16	192.61
	20100522	1339.44	0.24	2.80	170.66
	20100624	1372.40	0.46	5.08	309.63
	20100704	1382.40	0.48	5.34	325.48
	20100718	1396.37	0.42	5.01	305.37
	20100830	1439.31	0.45	5.23	318.78
	20100221	1248.72	0.40	3.27	199.31
	20100411	1297.60	0.42	3.99	243.20
	20100415	1301.55	0.56	3.99	243.20
	20100604	1352.44	0.33	3.66	223.08
	20100707	1385.40	0.47	5.45	332.19

Figure 5.25 shows the profile variations of *HeI*  $\lambda$ 4388, 4471, 4921, *MgII*  $\lambda$ 4481, and *HeII*  $\lambda$ 4686 from 2008 to 2010. From Figure 5.25 we identified several kinds of variations: emission wings appeared at the blue and red sides of *HeI*  $\lambda$ 4471 and  $\lambda$ 4921 line profiles, in addition *HeI*  $\lambda$ 4471 had strongly blended with other lines; *MgII*  $\lambda$ 4481 shows a noisy profile; *HeII*  $\lambda$ 4686 and *HeI*  $\lambda$ 4388 clearly show a normal profile of photospheric line. The analyses of their *EW* and *FWHM* are depicted in Figures 5.26 and 5.27. The figures show that *HeII*  $\lambda$ 4686 had the most stable value among other photospheric lines, in which the value of *FWHM* and *EW* are in the range of 2.81 to 3.30 Å and from 0.15 to 0.25 Å, respectively, whereas *HeI*  $\lambda$ 4388 had a larger range of *FWHM*: from 2.81 to 4.37 Å and *EW*: from 0.32 to 0.48 Å. The more stable values in the *HeII*  $\lambda$ 4686 profile indicates that the line was not affected by the lines produced by the envelopes.

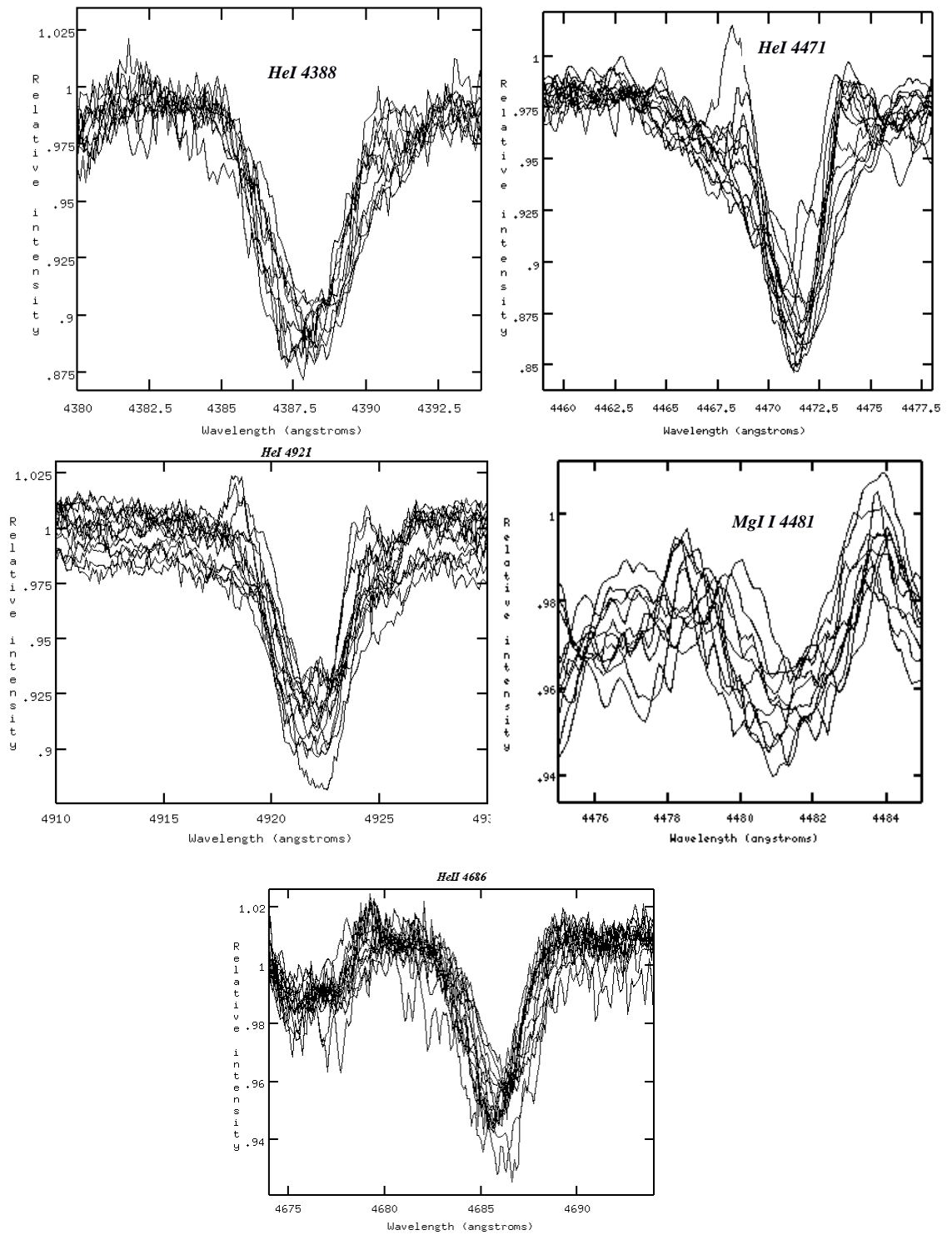


**Figure 5.25** – Profiles of photospheric lines in the blue region of  $\delta$ -Sco spectra from 2008 to 2010 observing runs. *HeII*  $\lambda$ 4686 was clearly not affected by the emission. There were emission wings on both sides of the profile of *HeI*  $\lambda$ 4921 and 4471.

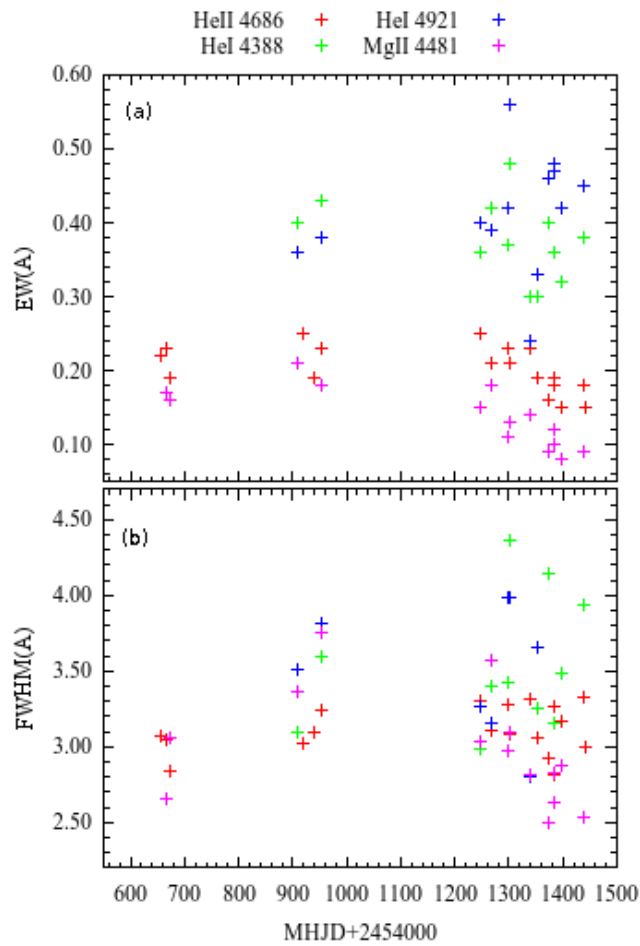


**Figure 5.26** – Variations of  $EW(a)$  and  $FWHM(b)$  of  $HeI\lambda 4388$ ,  $4921$ ,  $MgII\lambda 4481$ , and  $HeII\lambda 4686$  from 2008 to 2010.

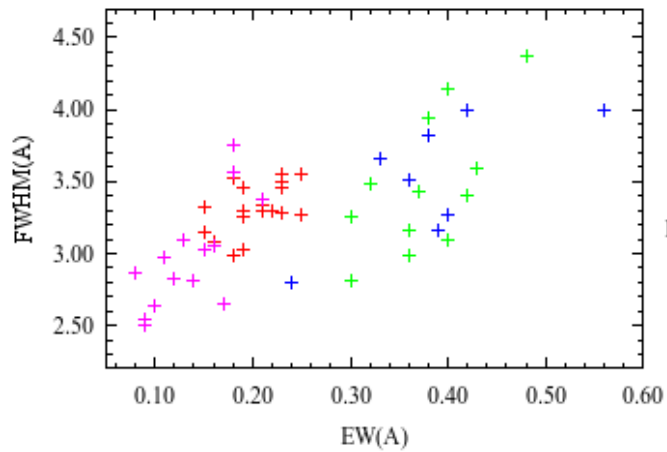


**Figure 5.27** – Correlation of  $FWHM$  and  $EW$  of  $HeI\lambda 4388$ ,  $4471$ ,  $4921$ ,  $MgII\lambda 4481$ , and  $HeII\lambda 4686$ . The graph also shows the variation of each line.  $HeII\lambda 4686$  was observed to be the least affected by the circumstellar envelope's lines.

We also correlated the behaviour of the line profiles in the circumstellar envelope and in the atmospheric regions. From the variation of  $EW$  in 2010, shown in Figure 5.28, the strength of  $H_\alpha$  and  $HeI \lambda 6678$  were gradually decreased, whereas  $HeII \lambda 4686$  and  $MgII \lambda 4481$  were slightly decreased. In contrast to  $HeI \lambda 4921$  and  $HeI \lambda 4388$ , neither of the lines showed any significant reduction; moreover, they have stronger  $EW$  values compared with the other photospheric lines. This is possibly because of effects from the circumstellar lines. In the meantime, the emitting region closer to the stellar surface,  $HeI \lambda 6678$ , shows a decrease in strength.

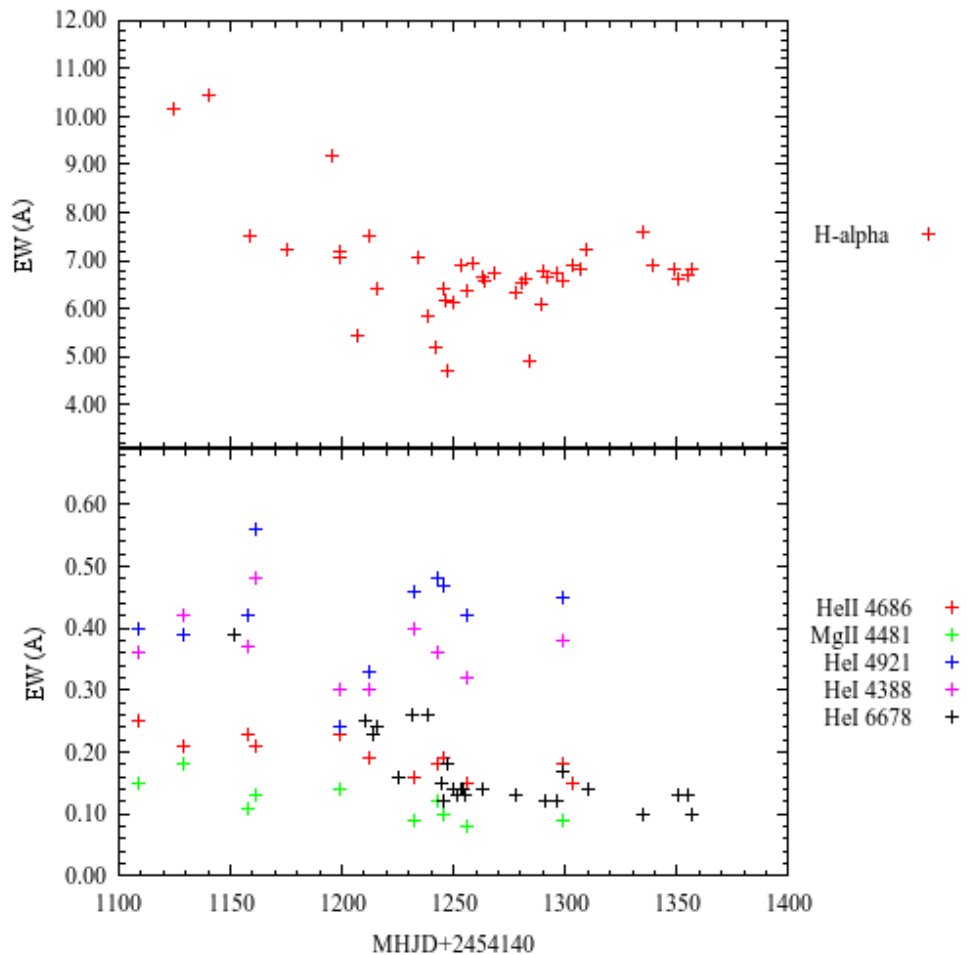


**Figure 5.28** – Variation of the line strength in the circumstellar envelope:  $H_\alpha$  and  $HeI \lambda 6678$  and photospheric lines:  $HeII \lambda 4686$ ,  $HeI \lambda 4921$ ,  $HeI \lambda 4388$ .

From chapter 2, we know that fast rotation is one of the characteristics of Be stars. The rotation model of Be stars was first proposed by Struve (1931), in which the instability produced by the rapid rotation leads to the ejection of material from the equatorial region of the flattened body of the star, forming a gaseous equatorial ring. We know that the value of *FWHM* has a relationship with the rotational velocity of the star and thus, the photospheric lines under study have been examined to determine the star's rotational velocity, especially when close to the periastron passage. The star is presumed to rotate at a constant value on its axis; thus, we expect the variation in the value of *FWHM* to be because of the condition in the local environment of the regions.

## 5.6 THE 2011 PERIASTRON PASSAGE OF $\delta$ -SCO

After the last periastron that occurred in 2000,  $\delta$ -Sco once again encountered the moment of its secondary at the closet distance to the primary. Many studies have been done to predict the date and physical parameters of the event. The distance of the primary and secondary at the periastron passage was estimated at 0.84 AU by Tango et al. (2009); Tycner et al. (2011) expected the periastron to occur on UT2011 July  $6 \pm 2$  days with an expected minimum separation of  $6.14 \pm 0.07$  mas (14 stellar radii).

### 5.6.1 *EW*, *I/Ic* and *V/R* variations

In this study, we analysed the line profiles in the circumstellar disc and the representative photospheric line, *HeII* 4686. We found the equivalent width of the Balmer lines:  $H_\alpha$ ,  $H_\beta$  and  $H_\gamma$ , were largely increased when the stars became closer to the periastron. The other lines, *HeI* $\lambda$  6678 and *HeIII* $\lambda$  4686 also revealed an increment in their strength but by smaller amount. Figure 5.29 shows the variation and the increment of the lines' strength when the stars were close to the periastron passage.